Electrochimica Acta 130 (2014) 200–205

Contents lists available at ScienceDirect

Electrochimica Acta

journal homepage: www.elsevier.com/locate/electacta

Anodic deposit from respiration metabolic pathway of *Escherichia coli*

Uyen Hoang Phuong Nguyen [a], Denys Grekov [a], Johannes Geiselmann [b], Valérie Stambouli [a], Marianne Weidenhaupt [a], Didier Delabouglise [a,*]

[a] *Laboratoire des Matériaux et du Génie Physique (LMGP), Grenoble Institute of Technology and CNRS, 3 parvis Louis Néel, CS 50257, 38016 Grenoble cedex 1, France*

[b] *Laboratoire Adaptation et Pathogénie des Microorganismes (LAPM), Université Joseph Fourier, Inserm and CNRS, Institut Jean Roget, BP 170, 38042 Grenoble Cedex 9, France*

ARTICLE INFO

Article history:
Received 14 November 2013
Received in revised form 28 February 2014
Accepted 2 March 2014
Available online 15 March 2014

Keywords:
E. coli
Bioelectrochemistry
Cyclic voltammetry
Redox mediator
Striping-deposition

ABSTRACT

Anaerobic incubation of *E. coli* K12 strains in an electrochemical cell induced the generation of an electrical current under constant polarization at 0.52 V/SHE. After incubation under potentiostatic conditions, the cyclic voltammetry signature points towards deposits of an insoluble layer of an oxidized redox compound. This bacterial redox mediator is soluble in its reduced state and exhibits a standard redox potential of 0.03 V/SHE at pH 7 with a slope of 120 mV per pH unit. A thorough inspection of the cyclic voltammetry allows us to shed light on how the bacteria interact with the electrode. Use of mutant strains of *E. coli* K12 in which genes of the synthetic pathways of ubiquinone and menaquinone were deleted did not interfere with the secretion of the redox mediator.

1. Introduction

Microbial fuel cells became a field of intense research after the initial discovery of electron transfer from bacteria, that otherwise naturally use an insoluble mineral oxide as final electron acceptor [1]. Three different mechanisms were suggested to explain the anodic activity of these bacteria: outer membrane cytochromes were discussed [2] as well as electrically conducting pili [3]. In fact, the electronic conductivity of pili could originate from structural arrangements of cytochromes [4]. Finally, the secretion into the medium of a natural redox shuttle was also clearly demonstrated [5]. Endogeneous redox molecules have thus become a key issue for understanding the electricity production of naturally occuring biofilms. Some studies have described a consortium effect, where a Gram-positive bacterium used phenazine derivatives produced by *Pseudomonas* as final electron acceptor of their respiratory chain [6]. Another recent example of bacterial mutualism was described in the characterization of an anodic biofilm in a bioelectrochemical system [7]: fermentative metabolites of *Enterobacter aerogens* stimulate the production of pyoacyanin by *Pseudomonas aeruginosa*. This phenazine-type molecule is effective for electron transfer and was subsequently used by *Enterobacter* as the final electron acceptor for their respiratory metabolism. This interaction increased the growth rate of the latter species and induced an even greater electrical current [7]. As shown by a survey of recent literature data, more phylogenetical strains than previously suspected possess the ability of inducing anodic electron transfer. In particular, *Escherichia coli* can produce an electrical current in microbial fuel cells without exogenous mediator [8]. Some authors suggested that *E. coli* secretes hydroquinones under electrochemical stimulation [9,10]. In other studies, different soluble molecules were proposed as possible electron carriers [11]. Here, we present a thorough electrochemical study of the anodic deposit produced by *E. coli* under potentiostatic conditions. A redox electron carrier accumulates on the anode during electrical current production. The reduced form of this mediator is more soluble and therefore diffuses more easily in the medium. We propose a possible interpretation of the current decrease in time observed in bacterial fuel cells using *E. coli*.

2. Materials and methods

2.1. Bacterial strains and media

E. coli K12 and its mutant derivatives in which either *ubi*C or *men*C are deleted, are described in ref 12. The gene *men*C codes for ortho-succinylbenzoate synthase, the enzyme catalyzing the aromatization step in the menaquinone synthesis pathway. The

* Corresponding author.
E-mail address: Didier.Delabouglise@phelma.grenoble-inp.fr (D. Delabouglise).

http://dx.doi.org/10.1016/j.electacta.2014.03.019
0013-4686/

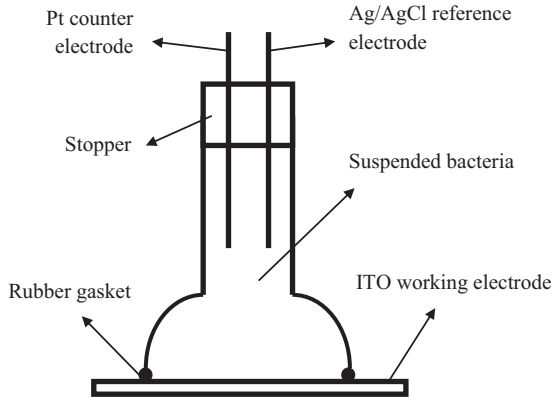

Fig. 1. Scheme of the electrochemical setup.

gene *ubi*C codes for chorismate pyruvate lyase, catalyzing the aromatization step in the ubiquinone synthesis pathway. Bacteria were grown in Luria-Bertani broth (Sigma-Aldrich) supplemented with the appropriate antibiotic (kanamycine) for one day. The stationary phase culture was centrifuged and washed twice with pure water. For electrochemical experiments, bacteria were re-suspended into minimal medium (M9, Sigma-Aldrich) containing Na_2HPO_4 (4.8 10^{-2} M), KH_2PO_4 (2.2 10^{-2} M), NaCl (8.5 10^{-3} M), NH_4Cl (1.8 10^{-2} M) and $MgSO_4$ (2 10^{-3} M). This medium was supplemented (1%) with a mineral mix containing per litre: 0.5 g of $MnCl_2.4H_2O$, 0.1 g of $FeSO_4.7H_2O$, 0.17 g of $Co(NO_3)_2.6H_2O$, 0.1 g of $ZnCl_2$, 0.04 g of $CuSO_4.5H_2O$, 0.05 g of $AlK(SO_4)_2.12H_2O$, 0.05 g of H_3BO_3, 0.01 g of $Na_2MoO_4.2H_2O$, 0.12 g of $NiCl_2$, 0.02 g $NaWO_4.2H_2O$, 0.1 g Na_2SeO_4. Glucose or sodium succinate were added as carbon sources (5 g.L^{-1}).

2.2. Electrochemical experiments

The electrochemical cell consisted of a tubular glass vessel (see Fig. 1). A plastic sheet (polyethylene terephtalate) covered by a conductive layer of Indium Tin Oxide (ITO, resistivity = 60 Ω/square, Sigma-Aldrich) was applied at the bottom of the vessel. The bacterial suspension was fluxed by argon for 15 min and the cell was then closed by a rubber stopper into which the counter electrode (platinum) and the reference electrode (silver covered by silver chloride) were inserted. All solid materials were previously sterilized by UV light for 15 min. The exposed working electrode surface area was 19.6 cm^2. The potential of the reference electrode was measured against a commercial electrode in minimal medium and was found to be 0.32 V/SHE (Standard Hydrogen Electrode). The cell was connected to a VMP2 potentiostat (Bio-Logic Sciences Instruments, Claix, France) and monitored by a computer running the EC-Lab software (Bio-Logic).

2.3. Scanning Electron Microscopy

After electrochemical experiments, the electrodes were imaged by Field Emission Gun Scanning Electron Microscopy (FEG - SEM) using a controlled pressure FEI Quanta FEG 250. To observe the bacteria adhering on the electrode surface, the plastic-ITO plates were cut into small sample pieces and fixed according to the following protocol:

- Fixation step: the electrode samples were immersed in a solution of glutaraldehyde 2% in sodium cacodylate buffer 0.1 M (pH 7.2) for 2 hours at 20 °C.
- Cleaning step: the electrode samples were cleaned three times with sodium cacodylate buffer 0.1 M (pH 7.2).
- Dehydratation step: the electrode samples were rinsed successively with ethanol 50%, 70% and 100%, for 20 min each. The electrode samples were then treated with hexamethyldisilazane and left to dry.

3. Results and discussion

For our experiments, we used a specific electrochemical cell in which the bacteria could gently sediment by gravity onto a polarized electrode used as an anode (Fig. 1). The bacteria were incubated in the electrochemical cell in a minimal medium at room temperature (see 2.1.) for several days, under an argon atmosphere. The bacterial concentration was adjusted initially to an optical density $OD_{600\ nm}$ = 0.2 to 0.3 (which corresponds roughly to 3 10^8 bacteria.mL^{-1}). During this step, the working ITO bottom electrode was continuously polarized at + 0.2 V against the reference (at + 0.52 V/SHE, see 2.2.). A typical current curve versus time of such an experiment is shown in Fig. 2. A relatively low, but significant current was observed. The current rose rapidly and passed through a maximum (0.5 ± 0.1 μA) during the ten first hours, then decreased progressively and stabilized on a plateau (near 0.1 μA) after about 35 hrs. The shape of this curve differed slightly with different experiments but in all cases exhibited a maximum between 6 and 10 h of experiment time. Cyclic voltammetries were performed just after the end of the potentiostatic experiment. Typical curves are shown in Fig. 3 (black lines). The initial voltammetric curves obtained at the beginning of the experiments are also shown (dotted lines, Fig. 3), in parallel with those obtained, for an identical setup, containing bacteria in an open circuit configuration (grey lines, Fig. 3). Another negative control was also performed in the absence of bacteria by applying the same potential to the same medium for several days. We obtained essentially in this case, the same curve as the dotted line in Fig. 3, except that slightly higher currents (- 0.04 mA at - 0.5 V) were observed for negative potentials, probably due to reduction of protons accumulated on the ITO electrode during anodic polarization. The relatively large electrical responses obtained during cyclic voltammetry after the potentiostatic experiment (black lines, Fig. 3) are therefore clearly related to bacterial activity. The prominent feature of these voltammetries is the large and coupled reductive and oxidative current appearing after potentiostatic incubation of the bacteria. A large cathodic signal (about–0.5 mA) appeared on the first cycle, indicating the reduction of a relatively large quantity of a chemical compound on the working electrode. On the reverse scan, an anodic wave culminated at a potential which is about 0.4 V above the maximum of the subsequent cathodic peak. The current decreased then slowly to reach a plateau on the positive portion of the diagram. On the second cycle, the intensity of the cathodic wave decreased steadily and its maximum was displaced by about 0.12 V towards anodic potentials. The intensity of the following anodic wave decreased accordingly but without any potential change. Further scans resulted in an asymptotic stabilization of the signals.

The voltammogram shape is typical of a striping-deposition process. During cathodic sweeps, the current increases when more negative potential values progressively allow overcoming the resistive effect of a reducible deposited layer. At the end of the dissolution of this deposit, the current drops abruptly. On the reverse scans, the anodic waves are of lower intensity and extended by a characteristic plateau corresponding to an increasing anodic overpotential due to the deposition of a poorly conducting oxidized phase. The cathodic current, as well as the anodic waves, sharply decrease on the second cycle and thereafter more smoothly, approaching an asymptotic value, in the following cycles. This is directly related to the cathodic dissolution of the reduced compounds and their diffusion into the entire volume of the electrolyte